

VARIABLE PARAMETER FREE ELECTRON LASER*

N. M. Kroll
University of California, San Diego
San Diego, California 92093

P. L. Morton
Stanford Linear Accelerator Center
Stanford University, Stanford, California 94305

and

M. N. Rosenbluth
Institute for Advanced Study
Princeton, New Jersey 08540

(Presented at the ONR Workshop on Electron Generators of Coherent Radiation, Telluride, Colorado, August 13-17, 1979.)

* Work supported in part by the Department of Energy under contract DE-AC03-76SF00515 and the Defense Advanced Research Projects Agency under contract MDA-903-78-0086.

1. INTRODUCTION

The recent successful operation of the "free electron laser" by the group at Stanford and the availability of high power electron beams has stimulated a great deal of interest in the use of the "free electron laser" (FEL) to produce a high power tunable laser beam.¹ It is the purpose of this paper to treat the FEL in a manner which has been used by accelerator physicists to treat the acceleration of charged particles with radio frequency accelerating systems.² This will allow us to use the ideas that have been developed for the acceleration of charged particles to guide us in the design of the wiggler magnet used for the FEL.

The emphasis of this paper is mainly tutorial so that the derivation of the equations are presented in a physically intuitive fashion rather than in a strictly rigorous manner.³ This type of treatment displays in a rather graphic way how the variation of the magnetic wiggler field and wave length affects the coupling of the electron energy to the optical laser beam. We will find that by proper variation of the wiggler parameters, it is possible to obtain a tremendous improvement in the performance of a variable parameter wiggler over the constant parameter wiggler.

2. EQUATIONS OF MOTION

(a) Derivation

We will consider the case where the wiggler magnet field and the signal (or optical field) may be derived from the vector potentials

$$\vec{A}_w = -(mc^2/e) a_w(z) \left[\hat{x} \cos\left(\int_0^z k_w(z_1) dz_1\right) + \hat{y} \sin\left(\int_0^z k_w(z_1) dz_1\right) \right] \quad (2.1)$$

and

$$\vec{A}_s = (mc^2/e) a_s(z) \left[\hat{x} \cos\left(\int_0^z k_s(z_1) dz_1 - \omega_s t\right) - \hat{y} \sin\left(\int_0^z k_s(z_1) dz_1 - \omega_s t\right) \right] \quad (2.2)$$

where we have introduced the dimensionless vector potentials $a = eA/mc^2$ ($E_0 = mc^2/e = .017 \text{ kG} \cdot \text{m} = .511 \text{ MV}$). Gaussian units will be used throughout this paper. We will assume that the fractional change in a_w and a_s is small over a distance of one wiggler period; i.e.,

$$\frac{d}{dz} (a) \ll k_w a \quad (2.3)$$

With this assumption and definition and the Lorentz equation

$$m\gamma(\ddot{\vec{x}} + \ddot{\vec{y}}) = e(\hat{x}E_x + \hat{y}E_y) - (ev_z/c)(\hat{x}B_y - \hat{y}B_x) \quad (2.4)$$

we obtain for the transverse velocity

$$\dot{\vec{x}} = \frac{c}{\gamma} \left\{ a_w(z) \cos\left(\int_0^z k_w(z_1) dz_1\right) - a_s(z) \cos\left(\int_0^z k_w(z_1) dz_1 - \omega_s t\right) \right\}$$

and

$$\dot{\vec{y}} = \frac{c}{\gamma} \left\{ a_w(z) \sin\left(\int_0^z k_w(z_1) dz_1\right) + a_s(z) \sin\left(\int_0^z k_w(z_1) dz_1 - \omega_s t\right) \right\} \quad (2.5)$$

The rate of change in the energy of the electron is given by

$$\dot{\gamma} = (e/mc^2)(\dot{x}E_x + \dot{y}E_y) \quad (2.6)$$

which yields

$$\dot{\gamma} = -\frac{k_s c a_s a_w}{\gamma} \sin \left[\int_0^z (k_w(z_1) + k_s(z_1)) dz_1 - \omega_s t \right] \quad (2.7)$$

where we have neglected the term a_s^2 compared to $a_s a_w$. For the case of a 1 kG wiggler of 5 cm period and a signal wavelength of 10^{-4} cm, the electric field of the signal wave must be much less than 10^{12} V/m, or equivalently the optical power density must be much less than 6×10^{21} Watts/m². This constraint will be easily satisfied for the cases of interest.

We will use the energy parameter γ and the phase ψ defined by

$$\psi = \left[\int_0^z (k_w(z_1) + k_s(z_1)) dz_1 - \omega_s t \right] \quad (2.8)$$

as the coordinates in the equations of motion. The equation of motion for ψ is

$$\dot{\psi} = (k_w + k_s)\dot{z} - \omega_s \quad (2.9)$$

We use the fact that $\omega_s = k_s c$, $v^2 = v_x^2 + v_y^2 + v_z^2$, $v_x/v \ll 1$, $v_y/v \ll 1$ and the relativistic approximation, $(c-v) = (c/2\gamma^2)$ to obtain

$$\dot{\psi} = c \left\{ k_w - \frac{k_s}{2\gamma^2} (\mu^2 - 2a_w a_s \cos \psi) \right\} \quad (2.10)$$

where

$$\mu^2 = \left(1 + a_w^2 + a_s^2 \right) \quad (2.11)$$

We will change the independent variable from t to z by using the condition that $dz = \dot{z} dt \approx c dt$, and obtain for the equations of motion

$$\psi' = k_w - \frac{k_s}{2\gamma^2} [\mu^2 - 2a_w a_s \cos \psi] \quad (2.12)$$

and

$$\gamma' = - \frac{k_s a_s a_w}{\gamma} \sin \psi \quad (2.13)$$

where the prime denotes the derivative with respect to longitudinal position z , along the wiggler. For completeness we need the equations that describe the signal field a_s and the wave number k_s as a function of z . The formula that describes the amplitude of the signal field may be obtained by observing that the energy lost by the electrons increases the energy in the optical field. This yields the following expression

$$a_s^2(z) = a_s^2(0) - \frac{Z_0 J}{k_s^2 E_0} [\bar{\gamma}(z) - \bar{\gamma}(0)]$$

or

$$a_s^2(z) = a_s^2(0) - \frac{\omega_p^2}{2\omega_s} [\bar{\gamma}(z) - \bar{\gamma}(0)] \quad (2.14)$$

where J is the current density of the beam, Z_0 is the impedance of free space, ω_p is the plasma frequency, and the bar over γ indicates the average over all of the electrons.

An alternative derivation of Eq. (2.14) along with the determination of δk_s is presented in Appendix I. The results derived there are

$$\delta k_s = \frac{\omega_p^2}{2c\omega_s} \frac{a_w}{a_s} \overline{\left(\frac{\cos \psi}{\gamma}\right)}$$

$$a'_s = \frac{\omega_p^2}{2\omega_s c} a_w \overline{\left(\frac{\sin \psi}{\gamma}\right)}$$

or

(2.15)

$$\delta k_s = \frac{a'_s}{a_s} \frac{\overline{(\cos \psi/\gamma)}}{\overline{(\sin \psi/\gamma)}}$$

With the previous assumption for the rate of change for a_s , Eq. (2.3), we see that it is possible to ignore the change in the wave number k_s and assume that $k_s \equiv \omega_s/c$. In deriving Eqs. (2.12) to (2.15) we have assumed that the cross section of the optical wave and the electrons are equal so that all of the electrons are coupled to the total optical wave. If the electron cross section is less than the cross section of the optical wave, we must multiply the current density J in Eq. (2.4) by a filling factor equal to the ratio of the beam cross section to optical wave cross section. Similarly, if the beam cross section is larger than the wave cross section, Eqs. (2.12) and (2.13) will be valid only for those electrons inside of the optical wave so that the average of γ over all particles is reduced. We will not belabor this point and for simplicity will assume that we are considering only the portion of electrons and optical wave that overlap.

The equations of motion derived above (Eqs. (2.12) and (2.13)) are valid (under the special assumptions that were made) for every electron, and given the initial conditions $\psi(0)$ and $\gamma(0)$ for every electron along

with the expressions for k_w , a_w , and a_s , these equations may be integrated to yield the values of ψ and γ as functions of the longitudinal position z . Of course, for a high gain FEL it is necessary to make sure that the signal field a_s used in the equations of motion is also a self consistent solution to Eqs. (2.14) or (2.15); by using a computer one can solve the equations of motion for a large number of particles and obtain the final coordinates in phase space for every particle as well as the final signal field and phase. In principle this procedure could be used to choose the optimum functional form for $k_w(z)$ and $a_w(z)$. It is possible to gain physical insight into the content of these equations without the need of integrating the equations of motion for a large number of initial conditions by referring the electrons energy variable γ to the synchronous or resonant value γ_r . This approach is extremely useful in determining the functions $k_w(z)$ and $a_w(z)$ to be used in different modes of operation for the FEL.

(b) Definition of Synchronous Energy and Phase

We first define the synchronous energy, γ_r , by

$$\gamma_r^2(z) = \frac{k_s \mu^2}{2k_w(z)} \quad (2.16)$$

and define the synchronous phase, ψ_r , by

$$\frac{d}{dz} (\gamma_r(z)) = - \frac{k_s a_w a_s}{\gamma_r} \sin \psi_r \quad (2.17)$$

Note that one is restricted in the choice for the function γ_r , since ψ_r is undefined if

$$\left| \frac{d\gamma_r}{dz} \right| > \left| \frac{k_s a_w a_s}{\gamma_r} \right| \quad (2.18)$$

It is possible to look at Eqs. (2.16) and (2.17) as definitions of γ_r and ψ_r assuming that k_w , a_w , and a_s are known functions of z . However, it is also possible to consider these as design equations where the wiggler functions k_w and a_w are to be determined to achieve the desired functions γ_r , ψ_r , and a_s .

Many of the other papers in this session will deal with different ways to choose ψ_r and γ_r and hence the wiggler parameters for various operating modes of the FEL. We first must study the motion of electrons with phase coordinates different from the synchronous values and demonstrate that for sufficiently small deviations the electrons will perform stable oscillations about the synchronous values; while, as we will see later, electrons with phase coordinates that are too far away from the synchronous values may be unstable and not oscillate about the synchronous values.

For the special case where we choose $\gamma_r = \text{constant}$, $\psi_r \equiv 0$ and we obtain from Eq. (2.16) that k_w and a_w are related by

$$k_w = \frac{k_s}{2\gamma_r^2} [1 + a_w^2] \quad (2.19)$$

where we have neglected a_s compared to a_w . This is the resonant condition one obtains for the standard constant parameter FEL.

(c) Motion About the Synchronous Energy

In this section we study the motion of the electrons about the synchronous energy by writing

$$\gamma = \delta\gamma + \gamma_r \quad (2.20)$$

with the definitions for γ_r and ψ_r as chosen in Eqs. (2.16) and (2.17), and with the assumption of $|\delta\gamma| \ll \gamma_r$, we can neglect the (a_s/a_w) terms to obtain the following equations of motion

$$\psi' = 2 \frac{k_w}{\gamma_r} (\delta\gamma) \quad (2.21)$$

and

$$(\delta\gamma)' = - \frac{k_s a_w a_s}{\gamma_r} (\sin \psi - \sin \psi_r) \quad (2.22)$$

These equations of motion may be obtained from the following Hamiltonian ⁴

$$H = \frac{k_w}{\gamma_r} (\delta\gamma)^2 + F(\psi) \quad (2.23)$$

where

$$F(\psi) = - \frac{k_s a_w a_s}{\gamma_r} (\cos \psi + \psi \sin \psi_r) \quad (2.24)$$

is the z dependent potential and for $\psi_r > 0$ is shown in Fig. 2.1.

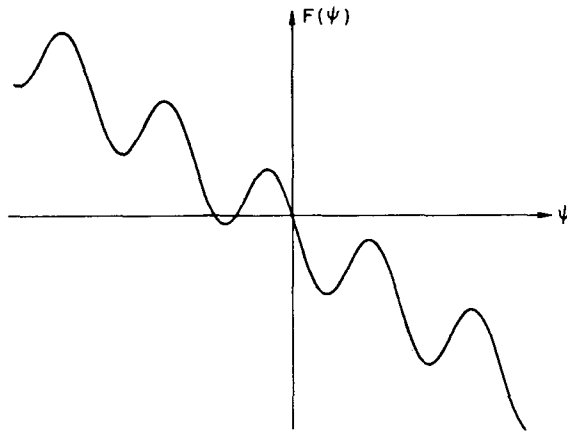


Fig. 2.1. Potential $F(\psi)$ versus ψ .

Of particular interest are design parameters chosen so that electrons trace out trajectories in the $\psi, \delta\gamma$ phase plane given by

$$\delta\gamma(\bar{H}, \psi, z) = \pm \sqrt{\frac{\gamma_r}{k_w} [\bar{H} - F(\psi)]} \quad (2.25)$$

where $\bar{H}(0)$ is given by the value of the Hamiltonian for the initial values of ψ and $\delta\gamma$. The closed orbits correspond to the electrons trapped in buckets and which perform stable oscillations about the synchronous value. If the change of parameters with z is adiabatic the $\bar{H}(z)$ is determined from $\bar{H}(0)$ and the requirement that the area of the closed phase curve, given by

$$J = \oint (\delta\gamma) d\psi \quad (2.26)$$

remains constant. Because the pattern repeats in ψ at intervals of 2π , we only will need to study the phase plane for $-\pi < \psi < \pi$. The maximum stable phase curve or bucket is shown in Fig. 2.2 and corresponds to

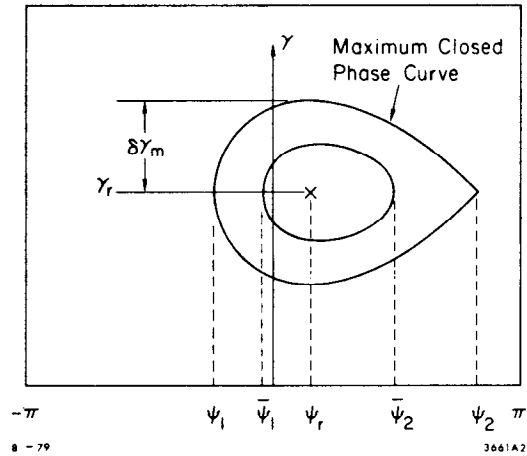


Fig. 2.2. Phase curves $\delta\psi$ versus ψ .

$$\bar{H}_m = \frac{k_s a_w a_s}{\gamma_r} \left[\cos \psi_r - (\pi \operatorname{sgn} \psi_r - \psi_r \sin \psi_r) \right] \quad (2.27)$$

while the maximum value of $\delta\gamma$ for which a particle may be trapped in a bucket is

$$\delta\gamma_m = \frac{2\gamma_r \sqrt{a_w a_s}}{\mu} \Gamma(\psi_r) \quad (2.28)$$

with

$$\Gamma(\psi_r) = \sqrt{\cos \psi_r - \left(\frac{\pi}{2} \operatorname{sgn} \psi_r - \psi_r \right) \sin \psi_r} \quad (2.29)$$

In the absence of prebunching, electrons will enter the wiggler at arbitrary initial phase ψ_0 . For electrons of energy γ_r , trapped electrons will oscillate between $\bar{\psi}_1$ and $\bar{\psi}_2$ where one of the limits is given by ψ_0 and the other is related to it by

$$\cos \bar{\psi}_1 + \bar{\psi}_1 \sin \psi_r = \cos \bar{\psi}_2 + \bar{\psi}_2 \sin \psi_r = \cos \psi_0 + \psi_0 \sin \psi_r \quad ,$$

$$(2.30)$$

as shown in Fig. 2.2. The maximum stable range for ψ_0 is given by the bucket intercepts of the ψ axis with $\gamma = \gamma_r$, and is designated by ψ_1 and ψ_2 in Fig. 2.2.

$$\psi_2 = \pi \operatorname{sgn} \psi_r - \psi_r \quad (2.31)$$

and

$$\cos \psi_1 + \psi_1 \sin \psi_r = \cos \psi_2 + \psi_2 \sin \psi_r \quad (2.32)$$

The area of the bucket shown in Fig. 2.2 may be obtained from Eq. (2.25) and is given by

$$J = \frac{8\gamma_r \sqrt{2a_s a_w}}{\mu} \alpha(\psi_r) \quad (2.33)$$

where

$$\alpha(\psi_r) = \frac{\sqrt{2}}{8} \int_{\psi_1}^{\psi_2} \left[\cos \psi_r + \cos \psi - (\pi - \psi_r - \psi) \sin \psi_r \right]^{\frac{1}{2}} d\psi \quad (2.34)$$

The electron with a small oscillation amplitude will oscillate in the clockwise direction about the synchronous point at $\delta\gamma = 0$, and $\psi = \psi_r$ with frequency Ω . For linear motion the frequency is

$$\Omega = \frac{2k_w}{\mu} \sqrt{a_s a_w \cos \psi_r} = \frac{\sqrt{\cos \psi_r}}{\Gamma(\psi_r)} \left(\frac{\delta\gamma_m}{\gamma} \right) k_w \quad (2.35)$$

Since the independent variable is z , the unit for Ω is inverse length. In order to define the closed phase curves it has been assumed that the change in the Hamiltonian is small in a distance corresponding to one synchrotron oscillation period.

3. CONSTANT PARAMETER WIGGLER

While the subsequent talks will discuss the general case where the wiggler parameters vary with z , it is useful to show how the results of the previous section apply to the original mode of FEL operation which utilized a wiggler with fixed wave number k_w and field amplitude a_w .⁵ This mode is one in which

$$\psi_r = \text{constant} = 0 \quad (3.1)$$

and

$$\gamma_r^2 = \text{constant} = \frac{k_s \mu^2}{2k_w} \quad (3.2)$$

so that the Hamiltonian which describes the motion of the electrons is given by

$$H = \frac{k_w}{\gamma_r} (\delta\gamma)^2 - \frac{k_s a_w a_s}{\gamma_r} \cos \psi \quad (3.3)$$

At first glance it is a little difficult to understand how such a device can accelerate or decelerate electrons since the initial phase distribution will be uniform and electrons which are injected near the synchronous energy will have their energy oscillate about the synchronous value. The average energy will be equal to the synchronous energy which remains constant for a non-accelerating bucket.

The key to the successful standard operation of the FEL is to inject the electrons above the synchronous energy and to allow the electrons to complete only a fraction of a synchrotron oscillation. An example of such an operation is shown in Fig. 3.1. Both electrons with an initial energy different from the resonant energy by an amount

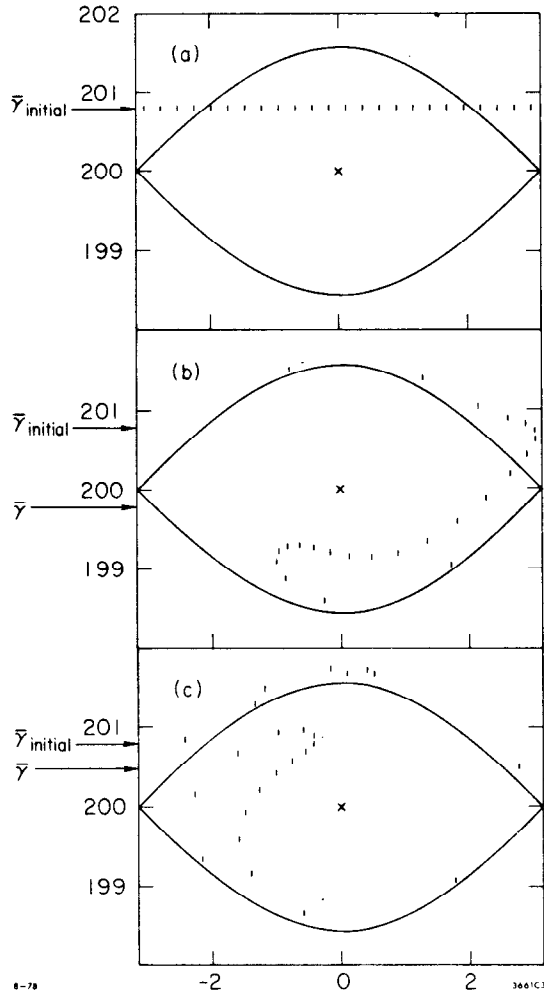


Fig. 3.1. Evolution of energy distribution of electrons. (a) Initial distribution. (b) After one-half oscillation. (c) After nearly one oscillation.

much larger than $\delta\gamma_m$ and electrons near the resonant energy will, on the average, have only a small energy charge. The electrons with the largest possible energy charge will have an initial energy $\delta\gamma_i \sim \delta\gamma_m$ as shown in Fig. 3.1a. After a distance L which corresponds to approximately one-half of a synchrotron oscillation, many electrons will have their energy shifted below the resonant energy as shown in Fig. 3.1b. For longer distances these electrons will continue to oscillate about the resonant energy and their initial energy will begin to increase

back to the initial energy as shown in Fig. 3.1c. From Eq.

(2.28) we see that the maximum

fractional energy loss is:

$$\left(\frac{\Delta\dot{\gamma}}{\gamma}\right)_{\text{max loss}} \sim \left(\frac{\delta\gamma_m}{\gamma}\right) = \frac{2\sqrt{a_w a_s}}{\mu} \quad (3.4)$$

while from Fig. 3.1b, we see that the electrons emerge with an energy spread

$$\left(\frac{\Delta\gamma}{\gamma}\right)_{\text{spread}} \sim \frac{\delta\gamma_m}{\gamma} \quad (3.5)$$

The optimum wiggler length L obtained from Eq. (2.35) is

$$L = \frac{\pi}{\Omega} = \lambda_w / 2 \left(\frac{\delta\gamma_m}{\gamma}\right) \quad (3.6)$$

with

$$\lambda_w \equiv \frac{2\pi}{k_w}$$

From Eqs. (3.4) and (3.6) we see that the maximum energy that can be extracted from the electron beam is inversely proportioned to the length of the wiggler, i.e.,

$$\left(\frac{\Delta\gamma}{\gamma}\right)_{\text{max loss}} \sim \frac{1}{2N} \quad (3.7)$$

where N is the number of wiggler periods, which results in either a low extraction rate or, for a large extraction rate, the need for a large ponderomotive potential term. A 10 kG wiggler with a 10 cm period gives $a_w \sim 10$, while an optical field of 10^8 w/cm^2 and 1 μm wave length gives $a_s \sim 10^{-5}$ so that a maximum fractional energy loss of $\sim 1\%$ with a $N=100$ wiggler is about the practical limit.

The fact that the average energy spread in the emerging electrons is equal or greater than the average energy loss places a severe restriction on the use of an FEL in a storage ring where repeated passages would quickly build up the energy spread in the beam until it exceeds either the storage ring acceptance or the width of the bucket.⁴ In the next section and in subsequent papers we will see how the variable wiggler schemes allows one to avoid these limitations.

4. PHASE AREA DISPLACEMENT

It is satisfying to note that the results of Section 2 give the correct answers for the constant parameter wiggler, however, the real use of the graphic method of buckets is in the understanding of FEL operation with variable parameters. In later talks the method of capturing a significant fraction of the electrons in a decelerating bucket will be discussed. This method is very useful for the case where the initial energy spread is small compared to the bucket size and can allow a large transfer of energy from the electron beam to the electrommagnetic wave.

In this section we would like to discuss a scheme of FEL operation that is much easier to understand with the aid of the moving bucket graphics.

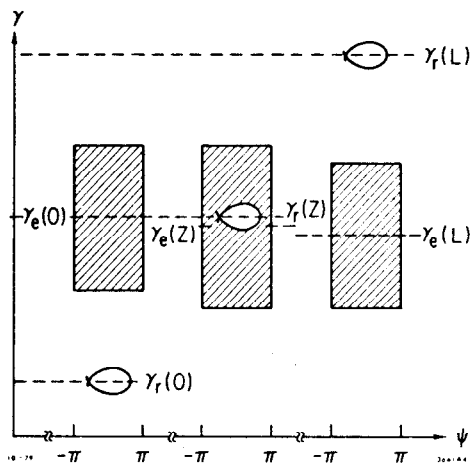


Fig. 4.1. Position of empty bucket and phase area of electron at various positions in the FEL.

The method called phase area displacement refers to an operational mode in which an empty bucket is accelerated through the phase area of the beam with the result that the phase area occupied by the electrons is displaced downward in energy.² This is illustrated in Fig. 4.1 where the accelerating bucket ($\psi_r < 0$) starts with a resonant energy far below the energy of the electrons and is adiabatically moved through the beam

until the final resonant energy is far above the electrons' energy. The final mean energy of the electrons is lowered by the phase area of the empty accelerating bucket divided by 2π , while the final energy spread of the beam is nearly equal to the initial energy spread, i.e.,

$$\langle \gamma(0) \rangle - \langle \gamma(L) \rangle = \frac{1}{2\pi} J \quad (4.1)$$

$$\Delta \gamma_f \sim \Delta \gamma_i \quad (4.2)$$

where J is the area enclosed by the accelerating bucket and is given by Eq. (2.33).

The method of phase area displacement can allow all of the electrons to be decelerated even when the initial energy spread (or effective energy spread when transverse emittance and magnetic field variation with beam size are included) is considerably larger than the bucket height. Indeed as long as the total change in γ_r is much larger than the sum of the bucket height and the energy spread in the beam, and the change is made adiabatically the average energy loss of the electron is independent of the initial energy spread in the beam. In order that the increase in the energy spread remain small it is necessary, in addition, to keep the phase area of the bucket constant during the displacement. Otherwise electrons displaced where the bucket area is larger will have their energy decreased more than those displaced where it is small.

The results of integrating the equations of motion (2.12) and (2.13) for a large number of particles with various initial energy spreads is presented in Figs. 4.2 and 4.3. The value of $\psi_r = -15^\circ$, the length of wiggler = 80 m, $\bar{\gamma}_{\text{initial}} = 200$, the wavelength and intensity of the electromagnetic radiation is $1 \mu\text{m}$ and $5 \times 10^9 \text{ W/cm}^2$. The average energy lost by an electron is plotted versus the initial energy spread of the

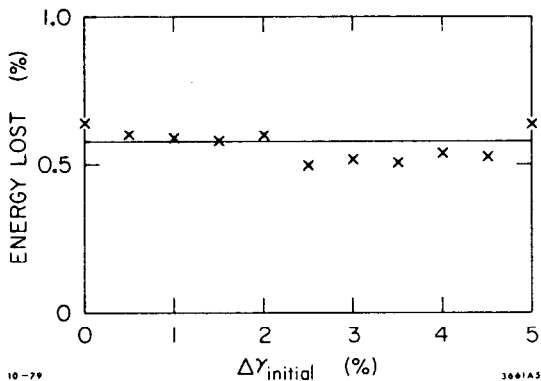


Fig. 4.2. Average energy lost.

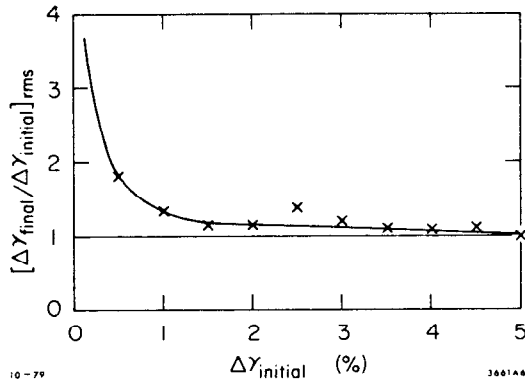


Fig. 4.3. Ratio of final/initial energy spread.

beam in Fig. 4.2, where we see that the average energy lost is nearly independent of the initial energy spread. In Fig. 4.3 we see that for large initial energy spreads the increase in the energy spread is quite small.

For the case where ψ_r is held constant a small fraction of the particles are often captured by the moving bucket and will have their energy increased, thereby significantly contributing to the increase in the energy spread of the final electron beam. The particles that may become captured are those which are near the unstable fixed point of the bucket. One method that may be used to prevent this capture is to increase the magnitude of the resonant phase angle ψ_r as the bucket is accelerated; this moves the unstable fixed point slightly preventing trapping of the electron. It also tends to decrease the phase area, so careful design is required to balance the virtue of constant bucket area against that of capture avoidance.

As a final example of the use of phase area displacement deceleration we have integrated the equations of motion (2.12) and (2.13) for the case where the same electron beam passes through the FEL many times.

We have assumed that between passages through the FEL all electrons have an equal energy added to replace energy lost to the electromagnetic wave, in addition the phase of each particle is randomized between passages. This simulates the case of an FEL in a storage ring where an rf cavity replaces the electron's energy loss. We have assumed an initial monoenergetic electron beam with $\gamma_{\text{initial}} = 200$, an electromagnetic wave of $1 \mu\text{m}$ with an intensity of $5 \times 10^9 \text{ W/m}^2$. The wiggler design is such that ψ_r changes from -15° to -27° in a length of 60 m. This corresponds to a change in the wiggler wavelength and magnetic field of

$$\lambda_w = 3.61 \text{ cm} \rightarrow 4.41 \text{ cm}$$

and

$$B_w = 3.42 \text{ kg} \rightarrow 4.19 \text{ kg} \quad .$$

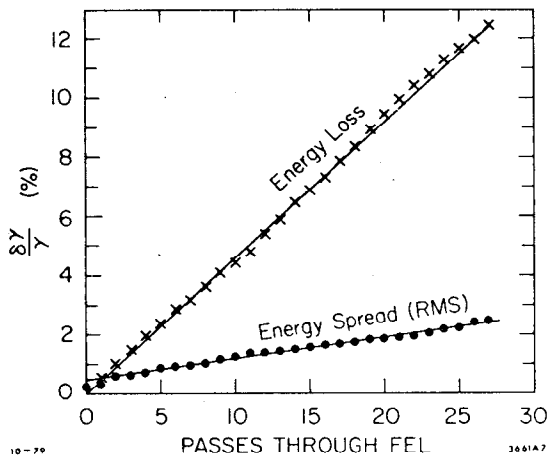


Fig. 4.4. Energy loss and spread of electron beam for multiple passes through an FEL.

In Fig. 4.4 we have plotted the average energy loss and the energy spread of the beam as a function of the number of passes through the FEL. We note that the build up rate from the energy spread is much slower than the rate of energy lost, whereas for the case of a constant parameter wiggler the build up of the energy spread is greater than the rate of energy

loss. Also for beams with energy spreads as large as 2% the electrons continue to lose energy at a reasonable rate.

5. CONCLUSION

In this report we have described the use of the graphical method with moving buckets to help design and understand various operational modes of the FEL. The importance of using the concept of buckets to describe the particle motion is not only useful for understanding of the various schemes but has proved to be very useful in the invention of these schemes.

6. REFERENCES

1. J. M. J. Madey, M. A. Schwettman and W. M. Fairbank, IEEE Trans. on Nucl. Sci. 20, 980 (1973).
2. K. R. Symon and A. M. Sessler, CERN Symposium 1956, 1, pp. 44-58.
3. See for example, N. Kroll, P. Morton and M. Rosenbluth, "Free Electron Laser with Variable Parameter Wiggler," submitted to Phys. Rev. A.
4. A. Bambini and A. Renieri, L. Pianore (versiglia), 17-30/16/1977.
5. W. B. Colson, "Physics of Quantum Electronics," Eds. by S. Jacobs, M. Sargent and M. Scully, 5, Ch. 4, Addison Wesley Publishing Co. (1978).

APPENDIX I

An alternative derivation of Eq. (2.14) along with a determination of δk_s can be obtained from the Maxwell equation

$$\frac{\partial^2 \underline{A}_s}{\partial z^2} - \frac{1}{c^2} \frac{\partial^2 \underline{A}_s}{\partial t^2} = -\frac{4\pi}{c} \underline{J}_1 \quad (\text{A.1})$$

Substitution of the form (2.2) yields

$$\frac{2\omega_s}{c} \delta k_s A_s \hat{e}_1 - \frac{2\omega_s}{c} A'_s \hat{e}_2 = \frac{4\pi}{c} \underline{J}_1 \quad (\text{A.2})$$

where \hat{e}_1 and \hat{e}_2 are defined by

$$\hat{e}_1 = \left[\hat{x} \cos\left(\int_0^z k_s(z_1) dz_1 - \omega_s t\right) - \hat{y} \sin\left(\int_0^z k_s(z_1) dz_1 - \omega_s t\right) \right]$$

$$\hat{e}'_1 = k_s \hat{e}_2 \quad (\text{A.3})$$

and we have neglected derivatives of A'_s and δk_s compared to ω_s/c .

Because \hat{e}_1 is a unit vector and $\hat{e}_1 \cdot \hat{e}_2$ vanishes we therefore find

$$\frac{2\omega_s}{c} \delta k_s A_s = \frac{4\pi}{c} \underline{J}_1 \cdot \hat{e}_1 \quad (\text{A.4})$$

In order that the form originally chosen for \underline{A}_s be strictly correct it is necessary that the right hand side of Eq. (A.4) be time independent. In actual fact the $\underline{J}_1 \cdot \hat{e}_1$ generated by the assumed form for \underline{A}_s will be a periodic function of time with period $2\pi/\omega_s$. We shall eliminate the oscillating terms by carrying out a long time average of $\underline{J}_1 \cdot \hat{e}_1$. Such

a procedure is valid* provided $\delta k_s \ll k_w$.

For a single electron we have

$$\underline{J}_1 \cdot \hat{e}_1 = e \underline{v}_1 \cdot \hat{e}_1 \delta(x - x_0(t)) \delta(y - y_0(t)) \delta(z - z_0(t)) \quad (\text{A.5})$$

where

$$\underline{v}_1 = \frac{-e\tilde{A}}{\gamma mc} \approx \frac{-e\tilde{A}_w}{\gamma mc} \quad (\text{A.6})$$

for $\tilde{A}_s \ll \tilde{A}_w$. Hence

$$\left(\underline{J}_1 \cdot \hat{e}_1 \right)_{\text{single particle}} = \frac{e^2 A_w^2(z)}{\gamma mc} \cos \psi \delta(x - x_0(t)) \delta(y - y_0(t)) \delta(z - z_0(t)) \quad (\text{A.7})$$

We time average by integrating over time from say $-T/2$ to $T/2$ to obtain

$$\begin{aligned} \left(\underline{J}_1 \cdot \hat{e}_1 \right)_{\text{single particle}} &= \frac{e^2 A_w^2(z)}{v_z T \gamma mc} \cos \psi(z) \delta(x - x_0(t(z))) \delta(y - y_0(t(z))) \\ &\quad \text{for } -T/2 < t(z) < T/2 \\ &= 0 \text{ otherwise} \end{aligned} \quad (\text{A.8})$$

Summing over all electrons, and average over the beam cross section to eliminate the transverse δ functions we obtain

$$\left(\underline{J}_1 \cdot \hat{e}_1 \right)_{\text{time average}} = \frac{n e^2 A_w^2}{mc} \overline{\left(\frac{\cos \psi}{\gamma} \right)} \quad (\text{A.9})$$

* The field produced by the higher harmonics is small because the higher harmonics are not phase matched. That is to say their phase velocity differs from c by too large an amount. The current will in general contain Fourier components of the general form $A_{ns}(z) \frac{\cos}{\sin} \left(n\psi \mp \int k_w dz \right)$, for which $(\omega/c - k)_n = (n \mp 1)k_w - n\delta k_s$. Thus a single term ($n-1$, with $n=1$) dominates so long as $\delta k_s \ll k_w$.

where again (—) means average over initial ψ and energy. Substitution of Eq. (A.9) with Eq. (A.4) yields

$$\delta k_s = \frac{\omega_p^2}{2c\omega_s} \frac{a_w}{a_s} \overline{\left(\frac{\cos \psi}{\gamma}\right)} \quad (\text{A.10})$$

Again from Eq. (A.2) we find

$$\frac{2\omega_s}{c} A'_s = -\frac{4\pi}{c} \mathbf{J}_{\sim 1} \cdot \hat{\mathbf{e}}_2$$

and proceeding in a similar manner we find

$$a'_s = \frac{\omega_p^2}{2\omega_s c} a_w \overline{\left(\frac{\sin \psi}{\gamma}\right)} \quad (\text{A.11})$$

To compare Eq. (A.11) with Eq. (2.14) we note that

$$\frac{dy}{dz} = -\frac{a_s a_w \omega_s}{c} \overline{\left(\frac{\sin \psi}{\gamma}\right)} \quad (\text{A.12})$$

The equivalence of Eq. (A.11) and Eq. (A.12) to Eq. (2.14) is apparent.

From Eq. (A.10) and Eq. (A.11) we have

$$\delta k_s = \frac{a'_s}{a_s} \overline{\frac{(\cos \psi/\gamma)}{(\sin \psi/\gamma)}} \quad (\text{A.13})$$

so that the assumption $a'_s/a_s \ll k_w$ made at the outset would appear to typically imply $\delta k_s \ll k_w$ as well. Since we expect the particles to bunch in the $0 < \psi < \pi/2$ range, $\overline{(\cos \psi/\gamma)}$ will be positive. This implies a tendency of the electron beam to trap the optical beam and hence to counter to some extent the effects of diffraction.